Supplementary Information Titles

Please list each supplementary item and its title or caption, in the order shown below.

Note that we do NOT copy edit or otherwise change supplementary information, and minor (nonfactual) errors in these documents cannot be corrected after publication. Please submit document(s) exactly as you want them to appear, with all text, images, legends and references in the desired order, and check carefully for errors.

Journal: Nature Medicine

Article Title:	**A human monoclonal antibody prevents malaria infection by targeting a new site of vulnerability on the parasite**
Corresponding Author:	Correspondence and requests for materials should be addressed to Marie Pancera (mpancera@fredhutch.org) or Robert A. Seder (rseder@mail.nih.gov)

Supplementary Item & Number **(add rows as necessary)**	Title or Caption
Supplementary Figure 1	**Binding specificity, *in vitro* inhibitory function and epitope mapping of PfCSP monoclonal antibodies.**
Supplementary Figure 2	**Apparent affinity of PfCSP antibodies by biolayer interferometry.**
Supplementary Figure 3	**Isothermal Titration Calorimetry (ITC) analysis of PfCSP antibodies.**
Supplementary Figure 4	**Crystal structures of CIS43 antigen-binding fragment in complex with PfCSP peptides and structural explanation for peptide 21 scanning mutagenesis.**
Supplementary Figure 5	**Binding specificity and functional capacity of antibody CIS43 variant (CIS43v).**
Supplementary Figure 6	**Crystal structures of CIS42 antigen-binding fragment in complex with PfCSP peptides.**
Supplementary Figure 7	**Structural comparison of peptide 21 bound to CIS43 and CIS42 antigen-binding fragments.**
Supplementary Figure 8	**Molecular Dynamics (MD) Simulations.**
Supplementary Figure 9	**Structural repeat motif analysis.**
Supplementary Figure 10	**Western blot used in Figure 5.**
Supplementary Figure 11	**Peptide 21 sequence conservation.**
Supplementary Table 1	**PfCSP immunoglobulin V-gene family usage.**

Nature Medicine: doi:10.1038/nm.4512

Supplementary Table 2	**Biolayer interferometry kinetics of PfCSP antibodies binding to rPfCSP, Peptide 21, or Peptide 29.**
Supplementary Table 3	**Data collection and refinement statistics for CIS43 antigen-binding fragment.**
Supplementary Table 4	**Details of the interactions of CIS43 antigen-binding fragment with peptides 20, 21, 25, and 29 (from Pisa web server).**
Supplementary Table 5	**Data collection and refinement statistics for CIS42 antigen-binding fragment.**
Supplemenatary Video 1	**Molecular dynamics simulation of free peptide 21, 500ns.**
Supplemenatary Video 2	**Molecular dynamics simulation of peptide 21 bound to CIS43 antigen-binding fragment, 500ns.**
Supplemenatary Video 3	**Molecular dynamics simulation of peptide 21 bound to CIS42 antigen-binding fragment, 500ns.**

Supplementary Information

Supplementary Figure 1 Binding specificity, *in vitro* inhibitory function and epitope mapping of PfCSP monoclonal antibodies.

a, Binding of varying concentrations of PfCSP antibodies isolated from plasmablasts to rPfCSP by ELISA. **b,** Effect of PfCSP antibodies on primary hepatocyte infection by PfSPZ *in vitro*. Infection rate was determined by enumeration of liver-stage parasites or exoerythrocytic forms (EEF) present at day 3.5 post infection and normalized by expressing as a fraction of untreated controls. Antibody concentrations are as shown, (bars represent mean EEF Fraction +/- one standard deviation). **c,** Binding specificity of PfCSP antibodies to rPfCSP, N-, Repeat, or C-terminal domains of PfCSP by ELISA. Controls: 2A10, a mouse antibody specific for the repeat region of PfCSP[22,23], and 5D5, a mouse antibody specific for the N terminus of PfCSP[37]. **d** and **e,** Binding of antibodies to overlapping peptides of PfCSP. (Right) Applies to **d** thru **g**, with specified amino acid sequences numbered 20–61 and color-coded representing overlapping peptides spanning the repeat region of PfCSP (residues 97–276). Peptides 28–41 and 46–60

consisted only of NANP repeats and are represented by peptide 29. **f and g,** Binding of PfCSP antibodies to rPfCSP in the presence of varying concentrations of peptides. Peptide color code as in **d**. Data are representative of two (**b**, **c**) or three (**a, d-g**) independent experiments.

Supplementary Figure 2 Apparent affinity of PfCSP antibodies by biolayer interferometry.

Avidity of PfCSP antibodies to: **a,** rPfCSP; **b,** Peptide 21; **c,** Peptide 29. Antibody binding curves are shown in black (raw data). Data were fitted (dotted red lines) with the binding equations describing a 1:1 heterologous ligand interaction. Serial concentrations of antibodies used are displayed on the panels of antibody CIS34. (n = 2, representative experiment is shown).

Supplementary Figure 3 Isothermal Titration Calorimetry (ITC) analysis of PfCSP antibodies.

Binding of PfCSP antibodies to rPfCSP or peptides. **a,** CIS23, CIS34, CIS42, mAb10. **b,** Binding of CIS43 to peptides 21 and 29. **c,** Binding of mAb10 to PfCSP mutant (PfCSP-P102A/D103N). Changes in the junctional epitope is depicted in red and highlighted in yellow. Upper panels show the output signal, dQ/dt, as a function of time. Lower panels show the integrated heats as a function of the antibody-site/rPfCSP molar ratio in the cell. The solid line represents the result from best non-linear least-squares fit of the data to a binding model that takes into account one or two sets of sites with different affinities. Dissociation constant (Kd), changes in Gibbs energy (ΔG) of binding, enthalpy (ΔH) and entropy (-TΔS) and stoichiometry (N) are shown. Data are representative of two independent experiments (**a**-**c**).

Supplementary Figure 4 Crystal structures of CIS43 antigen-binding fragment in complex with PfCSP peptides and structural explanation for peptide 21 scanning mutagenesis.

a, Surface representation of CIS43 antigen-binding fragment (light chain in wheat and heavy chain in light blue) with peptide 20, 21, 25, and 29 shown in sticks and colored as indicated. **b,** Surface representation of CIS43 antigen-binding fragment with 2Fo-Fc map shown at 1σ around peptide 21, with peptide removed for visualization, with hydrophobic residues (glycine, alanine, valine, leucine, isoleucine, proline, phenylalanine, methionine, and tryptophan) shown in orange and electrostatics. **c,** Ranking and structural explanation of peptide 21 alanine variants based on competition results from Fig. 3c. **d,** Structural visualization of the mutations. X indicates loss of hydrogen bonding when mutating the residue.

Supplementary Figure 5 Binding specificity and functional capacity of antibody CIS43 variant (CIS43v).

a, Amino acid sequence alignment of heavy chain variable regions of CIS43 and CIS43v. Mutations are shown in red. **b,** Binding of varying concentrations of CIS43 (solid lines) and CIS43v (dashed lines) to peptide 21 (magenta) and to rPfCSP (grey) by ELISA. Data are representative of two independent experiments. **c,** Binding free-energy changes (ΔΔG) of CIS43v antigen-binding fragment to peptide 21 were calculated for each individual mutation as well as for the four combined mutations. **d,** Effect of CIS43v on primary human hepatocyte infection by PfSPZ *in vitro*. Infection rate was determined as described in Fig. 2. Bars represent mean EEF +/- one standard deviation. Data are from one experiment for CIS43v (**d**).

Supplementary Figure 6 Crystal structures of CIS42 antigen-binding fragment in complex with PfCSP peptides.

a, Surface representation of CIS42 antigen-binding fragment (light chain in wheat and heavy chain in light green) with peptide 21 in magenta sticks representation and 90º rotation with view down towards the combining sites. Top row, surface representation of CIS42 antigen-binding fragment with peptides shown as sticks: peptide 21 (magenta), peptide 20 (green), peptide 25 (yellow) and peptide 29 (cyan). Bottom row, surface representation of CIS42 antigen-binding fragment with 2Fo-Fc electron density map shown at 1σ around peptide 21, with peptide removed for visualization, with hydrophobic residues (glycine, alanine, valine, leucine, isoleucine, proline, phenylalanine, methionine, and tryptophan) shown in orange and electrostatics. **b,** (Left) Details of the interactions of CIS42 antigen-binding fragment with the peptides. Antibody residues within 5 Å of the peptides are shown as sticks for the light (wheat) and heavy (light green) chains when bound to peptide 21, and as green, yellow and cyan for peptides 20, 25 and 29, respectively. (Right) Superposition of the peptides shown as sticks and colored as in **a** with sequences observed in electron density. **c,** Details of the interactions between peptide 21 and CIS42 antigen-binding fragment. Peptide 21 is shown in magenta as sticks representation. The CIS42 epitope is shown as sticks and semi-transparent surface with the residues colored based on the CDR regions for light chain in shades of wheat and for heavy chain in shades of green. **d,** Sequence of CIS42 antigen-binding fragment following Kabbat numbering with residues that contact each peptide shown as open star for side chains only, closed circle for main chain only and closed star for both main and side chains, colored under the sequences as in **a**. **e,** Sticks representation of peptide 21 (magenta) in the conformation bound to CIS42 antigen-binding fragment with superposition of three type-I β-turn NPNA repeat

structures of PfCSP as described in Ghasparian et al.[33]. Each NPNA repeat is labeled and shown in different colors for clarity. RMSD in Å is indicated over the total number of atoms used in the alignment.

Supplementary Figure 7 Structural comparison of peptide 21 bound to CIS43 and CIS42 antigen-binding fragments.

a, (Left) Side-by-side structural comparison of peptide 21 which adopts a different conformation when bound to CIS43 antigen-binding fragment (magenta) or CIS42 antigen-binding fragment (light pink) (residues do not align). (Right) 90º rotation showing the antibodies in transparent surface underlining a different angle of approach when binding to the peptide. **b,** Peptide 21 (magenta when bound to CIS43 antigen-binding fragment and light pink when bound to CIS42 antigen-binding fragment) aligned on the core NPN residues (residues 107-109) repeat region and angle of approach of the antibodies.

Supplementary Figure 8 Molecular Dynamics (MD) Simulations.

a, RMSD for CIS43 antigen-binding fragment bound to peptide 21over 500 nanoseconds (ns) of MD. CIS43 antigen-binding fragment heavy and light chain were used to align the trajectories. CIS43 antigen-binding fragment is depicted in indigo; full peptide 21 (residues 101-111) is depicted in plum; residues 107-109 in grape; and residues 101-103 in lavender. **b,** RMSD of CIS42 antigen-binding fragment bound to peptide 21 over 500 ns of MD, calculated the same as in **a**. CIS42 antigen-binding fragment is depicted in dark green; full peptide 21 (residues 101-113) is depicted in forest green; residues 107-109 in mint; and residues 101-103 in lime. **c,** RMSF of 500 ns of free peptide 21 beginning from its CIS43 antigen-binding fragment

conformation (depicted in magenta circles and a solid line) and RMSF of free peptide 21 beginning from its CIS42 antigen-binding fragment conformation (depicted in magenta squares with a dotted line). **d,** CIS43 and CIS42 antigen-binding fragment crystal structures aligned to their 500 ns frames respectively. Color key for CIS43 antigen-binding fragment: crystal heavy chain shown in purple and crystal light chain shown in gold; 500 ns heavy chain shown in lavender and 500 ns light chain shown in khaki. Color key for CIS42 antigen-binding fragment: crystal heavy chain shown in dark green and crystal light chain shown in sandy brown; 500 ns heavy chain shown in bright green and 500 ns light chain shown in yellow. **e,** Hydrogen bonding analysis of peptide 21 in complex with CIS42 and CIS43 antigen-binding fragments over 500ns compared to the respective crystal structures. Hydrogen bonds were calculated between peptide residues and the antigen-binding fragment binding interface. Numbers in parentheses indicate bonds present in the crystal structure. **f,** Principal component analysis (PCA) of 500 ns of free peptide 21 colored by the number of times specific conformations occur. PC1 is plotted on the x-axis and PC2 is plotted on the y-axis. Crystal structures of peptide 21 in CIS42 and CIS43 antigen-binding fragment conformations are labeled with gray arrows. The top ten eigen values from the PCA analyses are listed in the table. n = 50,000.

Supplementary Figure 9 Structural repeat motif analysis.

Phi and Psi angles (º) for residues N/D, P, N and A/V of the repeat motif for **a,** PfCSP peptides bound to CIS43 antigen-binding fragment; **b,** PfCSP peptides bound to CIS42 antigen-binding fragment; **c,** Average plus/minus one standard deviation for **a** and **b**; and **d,** Crystal structure of NPNA determined by Ghasparian et al.[33]. The alignment of the repeat motif peptide, based on the crystal structures as described in Fig. 4 and Supplementary Fig. 6, are shown as

indicated. The NPN repeat motif occurrences are underlined under the sequences. Highlighted in red are the notable outliers for which Phi and/or Psi is 60º different compared to others in the same row. For peptides bound to CIS43 antigen-binding fragment, this difference is in the first A/V, leading to a repeating structure of NPNA-NPNA; for peptides bound to CIS42 antigen-binding fragment, this difference is with N2 (the Asn following the Pro), leading to a repeating structure of ANPN-ANPN. We note that the Phi, Psi angles for the 1st occurrence of the NPN repeat in peptide 29 bound to CIS43 differs from the rest as shown in Fig. 4.

Supplementary Figure 10 Western blot used in Figure 5.

Concentrations (μg/ml) of monoclonal antibodies are indicated on top of the autoradiograph. Pulse, Chase, mAb15 (human anti-C terminus PfCSP antibody used as negative control); 5D5 (mouse anti-N terminus PfCSP antibody used as positive control for cleavage of PfCSP on PfSPZ); 43 (CIS43). Molecular mass is indicated in kilodaltons on the left side of the autoradiograph.

Supplementary Figure 11 Peptide 21 sequence conservation.

a, Complete PfCSP sequence of NF54 strain (clone 3D7). Central repeat region (in black) is flanked by the N- (blue) and C- (green) terminal regions, the leader (grey) and GPI anchor (orange) sequences. Boxed in magenta is peptide 21 sequence which occurs at the junction of the N- and Repeat regions. RI sequence is in brown letters. **b,** Peptide 21 sequence variation among laboratory and field isolates. Each residue within NF54 peptide 21 sequence is depicted with its position on top. Non-synonymous single nucleotide polymorphisms (SNPs) or indels leading to amino acid coding changes are shown with their respective frequencies, and geographic

locations. **c,** Pie chart representing frequencies of peptide 21 amino acid conservation shown in **b (**see URLs)[36,39-42].

Supplementary Table 1 PfCSP Immunoglobulin V-gene family usage.

Supplementary Table 2 Biolayer interferometry kinetics of PfCSP antibodies binding to rPfCSP, Peptide 21, or Peptide 29.

Supplementary Table 3 Data collection and refinement statistics for CIS43 antigen-binding fragment.

Supplementary Table 4 Details of the interactions of CIS43 antigen-binding fragment with peptides 20, 21, 25, and 29 (from Pisa web server).

Supplementary Table 5 Data collection and refinement statistics for CIS42 antigen-binding fragment.

Supplemenatary Video 1: Molecular dynamics simulation of free peptide 21, 500ns.

Simulation of free peptide 21 beginning from its CIS43-bound conformation. Peptide residues 101 – 111 are shown. Residues Asn_{107}, Pro_{108}, and Asn_{109} are colored in a gray backbone. Carbon atoms are depicted in cyan, nitrogen atoms in blue, and oxygen atoms in red.

Supplemenatary Video 2: Molecular dynamics simulation of peptide 21 bound to CIS43 antigen-binding fragment, 500ns.

The CIS43 antigen-binding fragment heavy chain is shown in purple and the light chain is shown in yellow. Key residues on the antigen-binding fragment involved in hydrogen bonding are shown in ball-and-stick: four amino acids on the heavy chain (Ala_{33}, Arg_{58}, Leu_{95}, and Leu_{98}) and one on the light chain (Tyr_{92}). Peptide residues 101 – 111 are shown in pink. Residues Asn_{107}, Pro_{108}, and Asn_{109}, which have been shown to be essential for binding, are colored in a gray

backbone. Carbon atoms are depicted in cyan, nitrogen atoms in blue, and oxygen atoms in red.

Supplemenatary Video 3: Molecular dynamics simulation of peptide 21 bound to CIS42 antigen-binding fragment, 500ns.

The CIS42 antigen-binding fragment heavy chain is shown in green and the light chain is shown in gold. Key residues on the antigen-binding fragment involved in hydrogen bonding are shown in ball-and-stick: four amino acids on the heavy chain (Thr_{31}, Asn_{52}, Tyr_{98}, and Gly_{99}) and one on the light chain (Ser_{27}). Peptide residues 101 – 111 are shown in pink. Residues Asn_{107}, Pro_{108}, and Asn_{109}, which have been shown to be essential for binding, are colored in a gray backbone. Carbon atoms are depicted in cyan, nitrogen atoms in blue, and oxygen atoms in red.

Nature Medicine: doi:10.1038/nm.4512

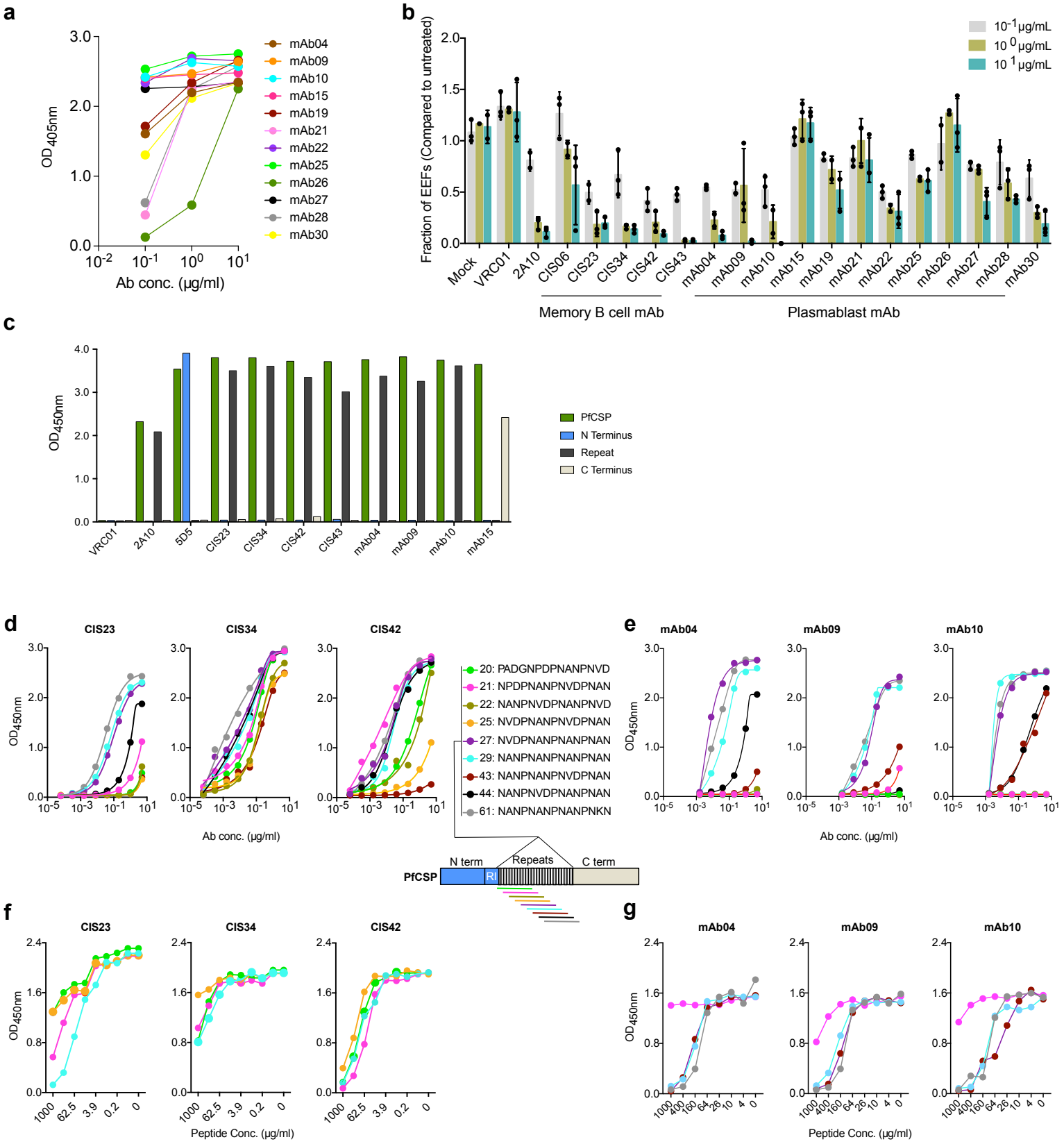

Supplementary Figure 1 Binding specificity, *in vitro* inhibitory function and epitope mapping of PfCSP monoclonal antibodies. **a,** Binding of varying concentrations of PfCSP antibodies isolated from plasmablasts to rPfCSP by ELISA. **b,** Effect of PfCSP antibodies on primary hepatocyte infection by PfSPZ in vitro. Infection rate was determined by enumeration of liver-stage parasites or exoerythrocytic forms (EEF) present at day 3.5 post infection and normalized by expressing as a fraction of untreated controls. Antibody concentrations are as shown, (bars represent mean EEF Fraction +/- one standard deviation). **c,** Binding specificity of PfCSP antibodies to rPfCSP, N-, Repeat, or C-terminal domains of PfCSP by ELISA. Controls: 2A10, a mouse antibody specific for the repeat region of PfCSP[20,21], and 5D5, a mouse antibody specific for the N terminus of PfCSP[35]. **d** and **e**, Binding of antibodies to overlapping peptides of PfCSP. (Right) Applies to **d** thru **g**, with specified amino acid sequences numbered 20-61 and color-coded representing overlapping peptides spanning the repeat region of PfCSP (residues 97-276). Peptides 28-41 and 46-60 consisted only of NANP repeats and are represented by peptide 29. **f** and **g**, Binding of PfCSP antibodies to rPfCSP in the presence of varying concentrations of peptides. Peptide color code as in **d**. Data are representative of two (**b, c**) or three (**a, d-g**) independent experiments.

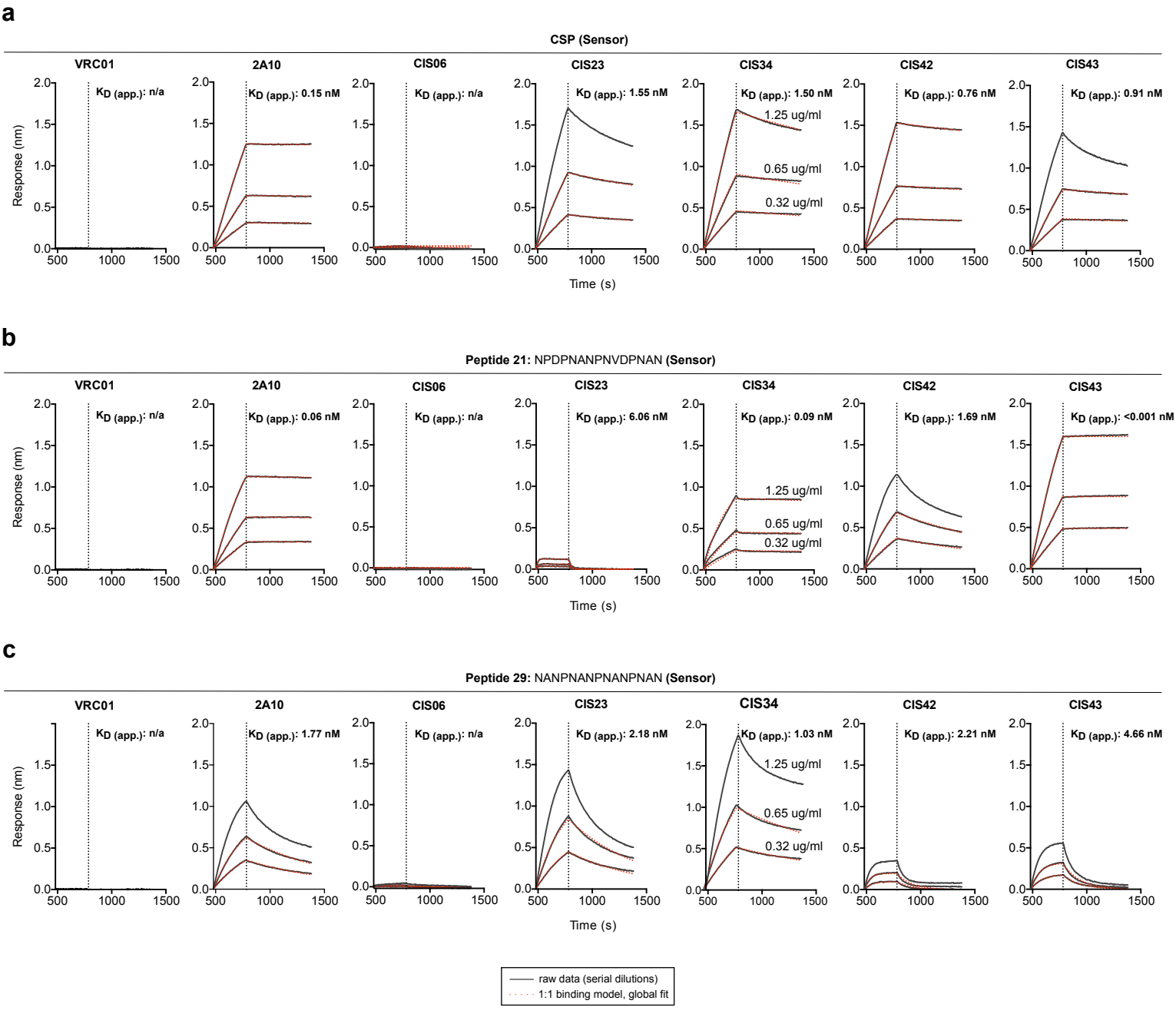

Supplementary Figure 2 Apparent affinity of PfCSP antibodies by biolayer interferometry.
Avidity of PfCSP antibodies to: **a,** rPfCSP; **b,** Peptide 21; **c,** Peptide 29. Antibody binding curves are shown in black (raw data). Data were fitted (dotted red lines) with the binding equations describing a 1:1 heterologous ligand interaction. Serial concentrations of antibodies used are displayed on the panels of antibody CIS34. (n = 2, representative experiment is shown).

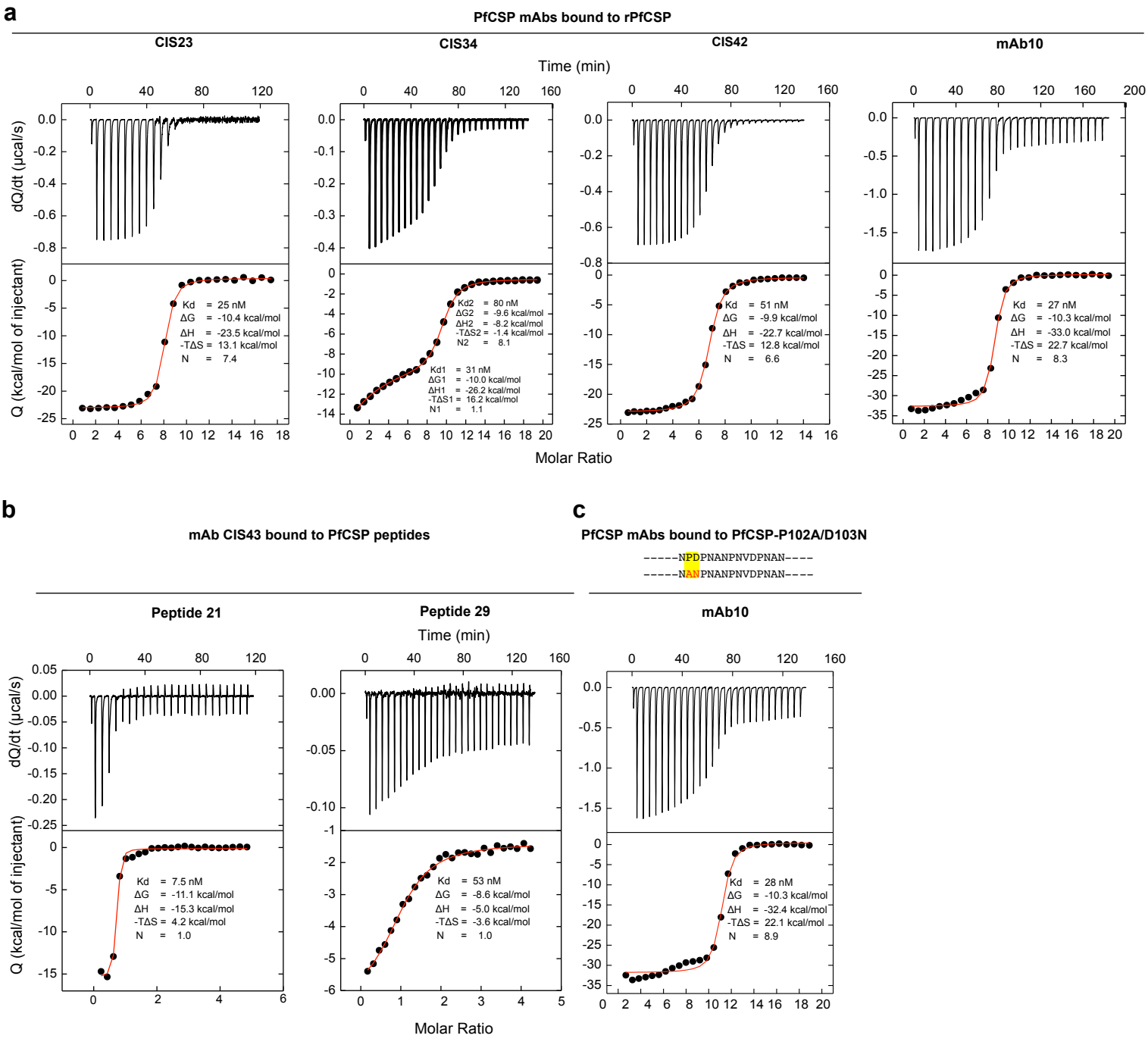

Supplementary Figure 3 Isothermal Titration Calorimetry (ITC) analysis of PfCSP antibodies.
Binding of PfCSP antibodies to rPfCSP or peptides. **a,** CIS23, CIS34, CIS42, mAb10. **b,** Binding of CIS43 to peptides 21 and 29. **c,** Binding of mAb10 to PfCSP mutant (PfCSP-P102A/D103N). Changes in the junctional epitope is depicted in red and highlighted in yellow. Upper panels show the output signal, dQ/dt, as a function of time. Lower panels show the integrated heats as a function of the antibody-site/rPfCSP molar ratio in the cell. The solid line represents the result from best non-linear least-squares fit of the data to a binding model that takes into account one or two sets of sites with different affinities. Dissociation constant (Kd), changes in Gibbs energy (ΔG) of binding, enthalpy (ΔH) and entropy (-TΔS) and stoichiometry (N) are shown. Data are representative of two independent experiments (**a-c**).

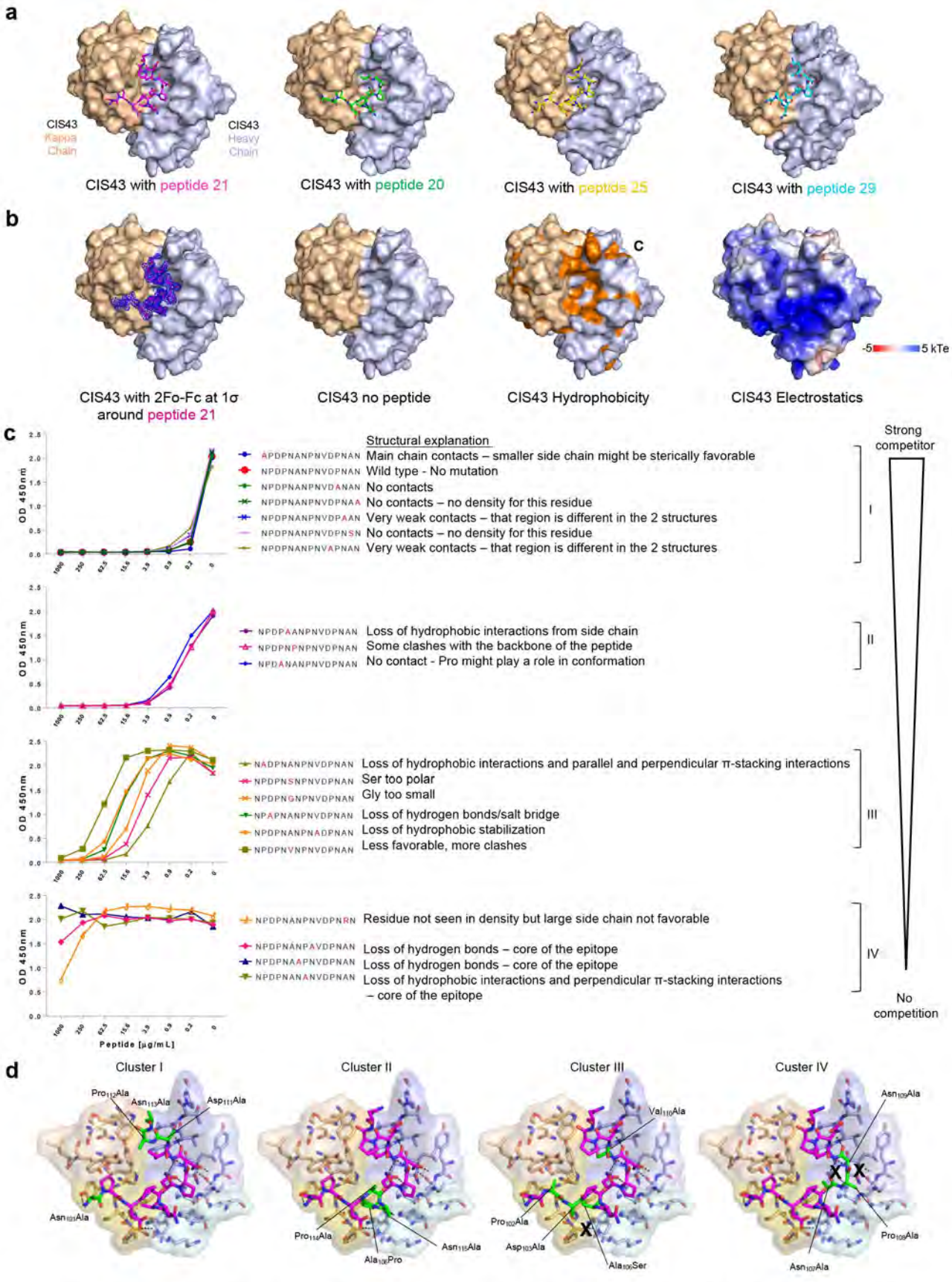

Supplementary Figure 4 Crystal structures of CIS43 antigen-binding fragment in complex with PfCSP peptides and structural explanation for peptide 21 scanning mutagenesis.

a, Surface representation of CIS43 antigen-binding fragment (light chain in wheat and heavy chain in light blue) with peptide 20, 21, 25, and 29 shown in sticks and colored as indicated. **b,** Surface representation of CIS43 antigen-binding fragment with 2Fo-Fc map shown at 1σ around peptide 21, with peptide removed for visualization, with hydrophobic residues (glycine, alanine, valine, leucine, isoleucine, proline, phenylalanine, methionine, and tryptophan) shown in orange and electrostatics. **c,** Ranking and structural explanation of peptide 21 alanine variants based on competition results from Fig. 3c. **d,** Structural visualization of the mutations. X indicates loss of hydrogen bonding when mutating the residue.

Nature Medicine: doi:10.1038/nm.4512

a

```
CIS43   Heavy  QVQLVQSGAEVKKPGASVKVSCKASGYTFTSYAIHWVRQA
CIS43v  Heavy  QVQLVQSGAEVKKPGASVKVSCKASGYTFTSYAIHWVRQA

CIS43   Heavy  PGQRLEWMGWIKAGNGNTRYSQKFQDRVTITRDTSTTTAY
CIS43v  Heavy  PGQRLEWMGWIKAGNGGGGYSGKFQDRVTITRDTSTTTAY

CIS43   Heavy  MELSSLRSEDTAVYYCALLTVLTPDDAFDIWGQGTMVTVSS
CIS43v  Heavy  MELSSLRSEDTAVYYCALLTVLTPDDAFDIWGQGTMVTVSS
```

b

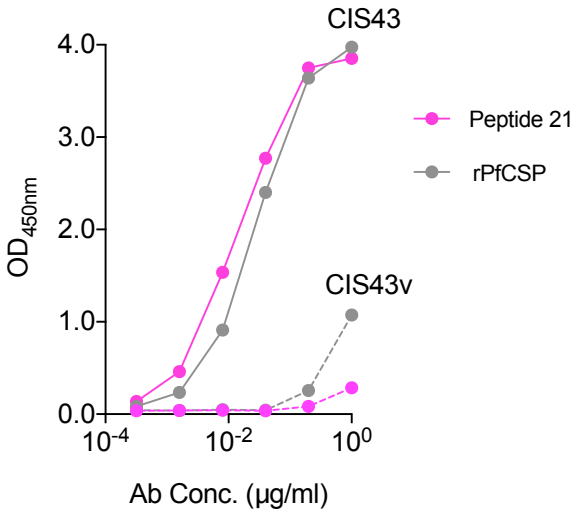

c

CIS43 variant	
Mutation	Binding free-energy changes (ΔΔG) (kcal/mol)
N56G	-0.01
T57G	-0.01
R58G	1.7
Q61G	0
N56G, T57G, R58G, Q61G	1.4

d

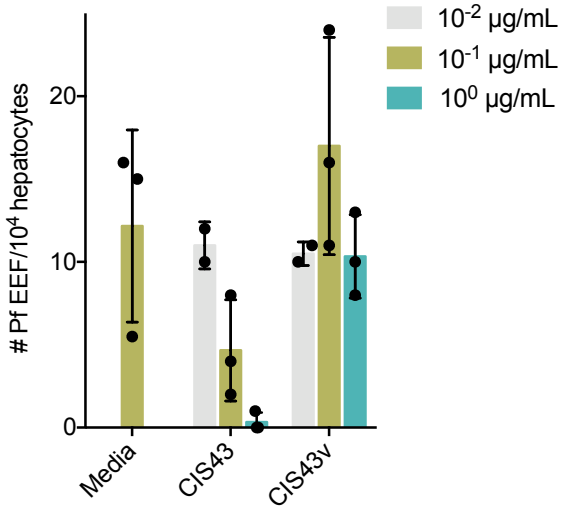

Supplementary Figure 5 Binding specificity and functional capacity of antibody CIS43 variant (CIS43v).
a, Amino acid sequence alignment of heavy chain variable regions of CIS43 and CIS43v. Mutations are shown in red. **b,** Binding of varying concentrations of CIS43 (solid lines) and CIS43v (dashed lines) to peptide 21 (magenta) and to rPfCSP (grey) by ELISA. Data are representative of two independent experiments. **c,** Binding free-energy changes (ΔΔG) of CIS43v antigen-binding fragment to peptide 21 were calculated for each individual mutation as well as for the four combined mutations. **d,** Effect of CIS43v on primary human hepatocyte infection by PfSPZ *in vitro*. Infection rate was determined as described in Fig. 2. Bars represent mean EEF +/- one standard deviation. Data are from one experiment for CIS43v (**d**).

Nature Medicine: doi:10.1038/nm.4512

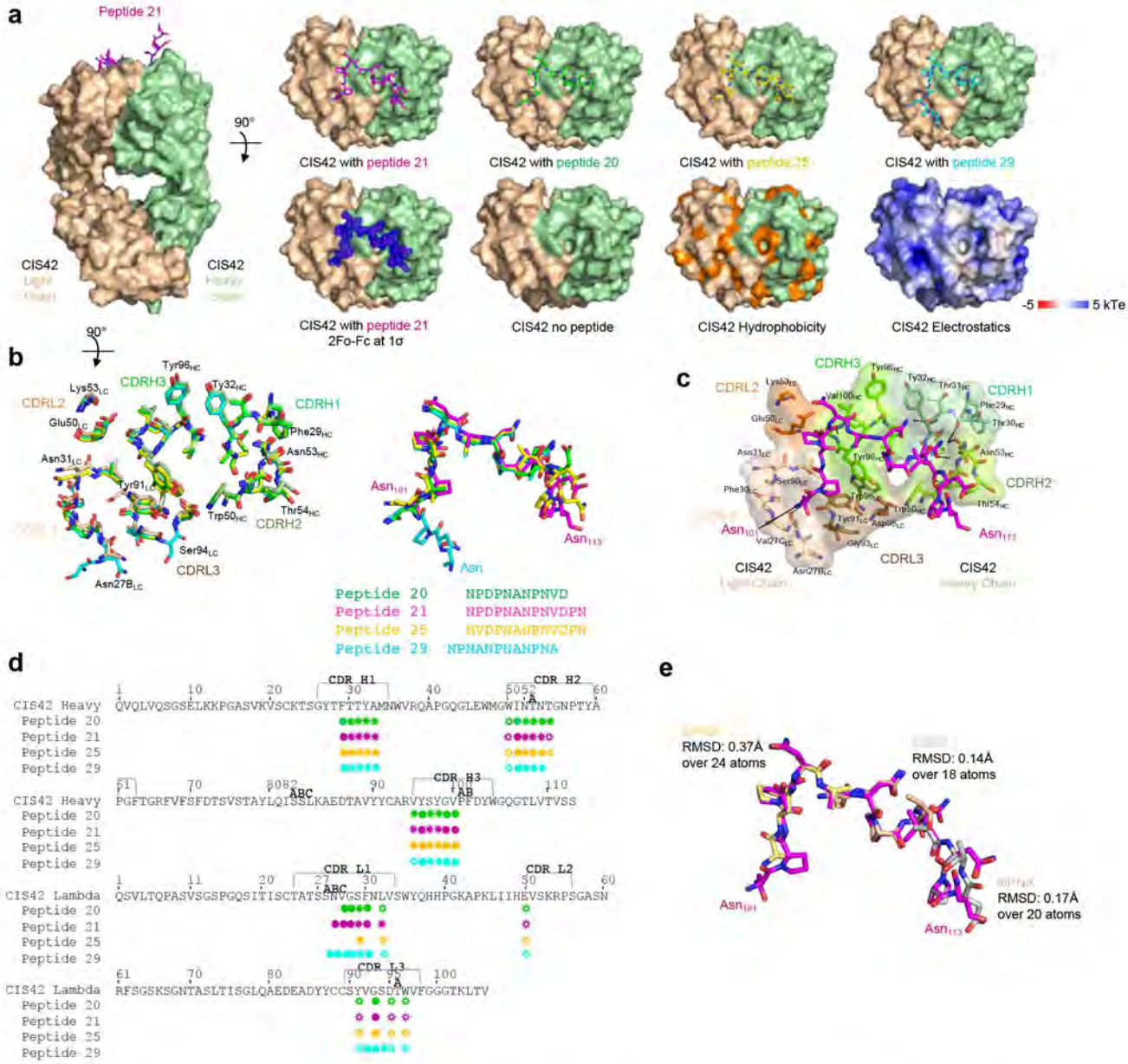

Supplementary Figure 6 Crystal structures of CIS42 antigen-binding fragment in complex with PfCSP peptides.
a, Surface representation of CIS42 antigen-binding fragment (light chain in wheat and heavy chain in light green) with peptide 21 in magenta sticks representation and 90° rotation with view down towards the combining sites. Top row, surface representation of CIS42 antigen-binding fragment with peptides shown as sticks: peptide 21 (magenta), peptide 20 (green), peptide 25 (yellow) and peptide 29 (cyan). Bottom row, surface representation of CIS42 antigen-binding fragment with 2Fo-Fc electron density map shown at 1σ around peptide 21, with peptide removed for visualization, with hydrophobic residues (glycine, alanine, valine, leucine, isoleucine, proline, phenylalanine, methionine, and tryptophan) shown in orange and electrostatics. **b,** (Left) Details of the interactions of CIS42 antigen-binding fragment with the peptides. Antibody residues within 5 Å of the peptides are shown as sticks for the light (wheat) and heavy (light green) chains when bound to peptide 21, and as green, yellow and cyan for peptides 20, 25 and 29, respectively. (Right) Superposition of the peptides shown as sticks and colored as in a with sequences observed in electron density. **c,** Details of the interactions between peptide 21 and CIS42 antigen-binding fragment. Peptide 21 is shown in magenta as sticks representation. The CIS42 epitope is shown as sticks and semi-transparent surface with the residues colored based on the CDR regions for light chain in shades of wheat and for heavy chain in shades of green. **d,** Sequence of CIS42 antigen-binding fragment following Kabbat numbering with residues that contact each peptide shown as open star for side chains only, closed circle for main chain only and closed star for both main and side chains, colored under the sequences as in **a**. **e,** Sticks representation of peptide 21 (magenta) in the conformation bound to CIS42 antigen-binding fragment with superposition of three type-I β-turn NPNA repeat structures of PfCSP as described in Ghasparian et al.[33]. Each NPNA repeat is labeled and shown in different colors for clarity. RMSD in Å is indicated over the total number of atoms used in the alignment.

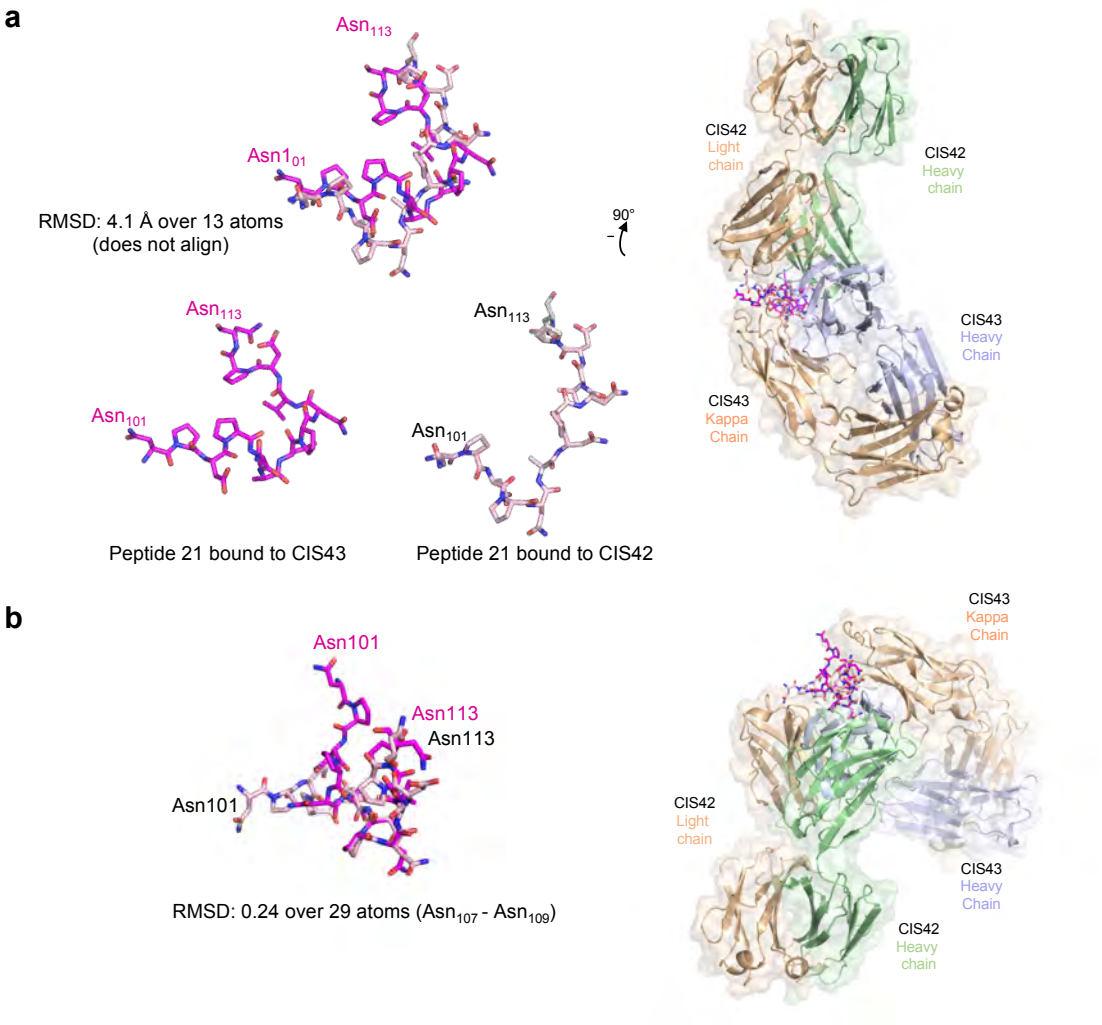

Supplementary Figure 7 Structural comparison of peptide 21 bound to CIS43 and CIS42 antigen-binding fragments. **a,** (Left) Side-by-side structural comparison of peptide 21 which adopts a different conformation when bound to CIS43 antigen-binding fragment (magenta) or CIS42 antigen-binding fragment (light pink) (residues do not align). (Right) 90º rotation showing the antibodies in transparent surface underlining a different angle of approach when binding to the peptide. **b,** Peptide 21 (magenta when bound to CIS43 antigen-binding fragment and light pink when bound to CIS42 antigen-binding fragment) aligned on the core NPN residues (residues 107-109) repeat region and angle of approach of the antibodies.

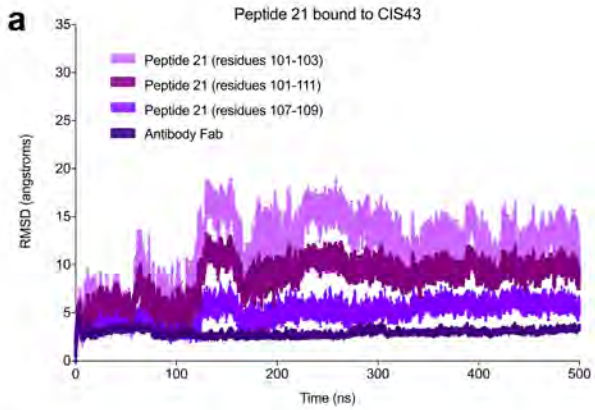

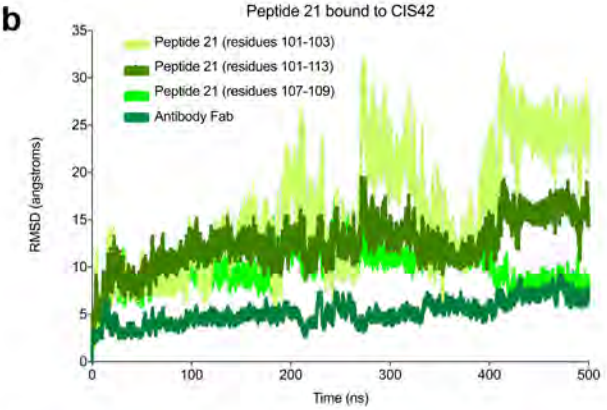

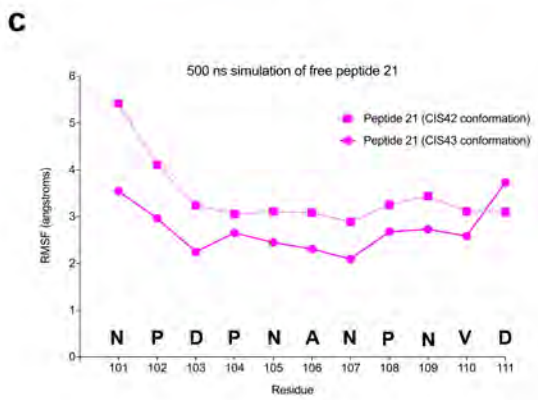

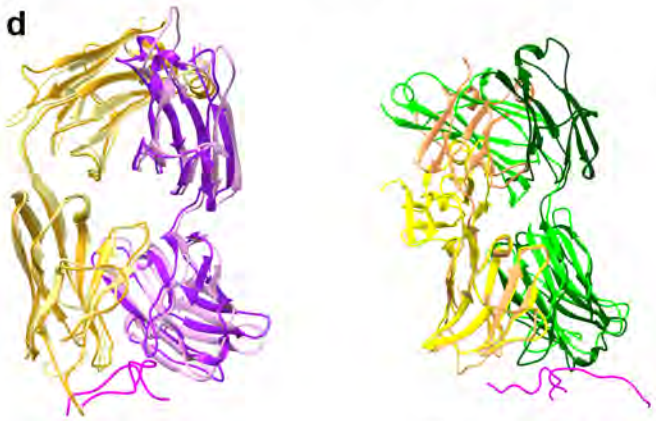

CIS43 bound to peptide 21
(crystal vs 500 ns)
2.96 Å RMSD

CIS42 bound to peptide 21
(crystal vs 500 ns)
7.48 Å RMSD

e

Time (ns)	CIS43 Fab	CIS42 Fab
	Number of hydrogen bonds	
Crystal	8	5
50	5 (3)	4 (1)
250	12 (2)	2 (0)
500	9 (1)	2 (0)

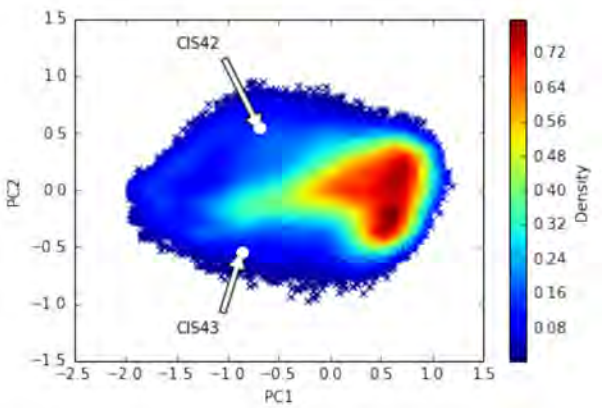

PC1	46.47
PC2	12.82
PC3	8.39
PC4	5.67
PC5	3.88
PC6	3.34
PC7	3.04
PC8	2.18
PC9	1.80
PC10	1.54

Supplementary Figure 8 Molecular Dynamics (MD) Simulations.
a, RMSD for CIS43 antigen-binding fragment bound to peptide 21over 500 nanoseconds (ns) of MD. CIS43 antigen-binding fragment heavy and light chain were used to align the trajectories. CIS43 antigen-binding fragment is depicted in indigo; full peptide 21 (residues 101-111) is depicted in plum; residues 107-109 in grape; and residues 101-103 in lavender. **b,** RMSD of CIS42 antigen-binding fragment bound to peptide 21 over 500 ns of MD, calculated the same as in a. CIS42 antigen-binding fragment is depicted in dark green; full peptide 21 (residues 101-113) is depicted in forest green; residues 107-109 in mint; and residues 101-103 in lime. **c,** RMSF of 500 ns of free peptide 21 beginning from its CIS43 antigen-binding fragment conformation (depicted in magenta circles and a solid line) and RMSF of free peptide 21 beginning from its CIS42 antigen-binding fragment conformation (depicted in magenta squares with a dotted line). **d,** CIS43 and CIS42 antigen-binding fragment crystal structures aligned to their 500 ns frames respectively. Color key for CIS43 antigen-binding fragment: crystal heavy chain shown in purple and crystal light chain shown in gold; 500 ns heavy chain shown in lavender and 500 ns light chain shown in khaki. Color key for CIS42 antigen-binding fragment: crystal heavy chain shown in dark green and crystal light chain shown in sandy brown; 500 ns heavy chain shown in bright green and 500 ns light chain shown in yellow. **e,** Hydrogen bonding analysis of peptide 21 in complex with CIS42 and CIS43 antigen-binding fragments over 500ns compared to the respective crystal structures. Hydrogen bonds were calculated between peptide residues and the antigen-binding fragment binding interface. Numbers in parentheses indicate bonds present in the crystal structure. **f,** Principal component analysis (PCA) of 500 ns of free peptide 21 colored by the number of times specific conformations occur. PC1 is plotted on the x-axis and PC2 is plotted on the y-axis. Crystal structures of peptide 21 in CIS42 and CIS43 antigen-binding fragment conformations are labeled with gray arrows. The top ten eigen values from the PCA analyses are listed in the table. n = 50,000.

Supplementary Table 5 Data collection and refinement statistics for CIS42 antigen-binding fragment.

	CIS42 Fab with peptide 20	CIS42 Fab with peptide 21	CIS42 Fab with peptide 25	CIS42 Fab with peptide 29
Data collection				
Space group	$P2_12_12_1$	$P2_12_12_1$	$P2_12_12_1$	$P2_12_12_1$
Cell dimensions				
a, *b*, *c* (Å)	41.83, 70.68, 166.73	41.13, 70.57, 165.34	41.96, 70.82, 164.9	41.58, 70.67, 163.36
α, β, γ (°)	90.0, 90.0, 90.0	90.0, 90.0, 90.0	90.0, 90.0, 90.0	90.0, 90.0, 90.0
Resolution (Å)	50-2.30 (2.48-2.43, 2.43-2.38, 2.38-2.34, 2.34-2.30)*	50-1.77 (1.95-1.91, 1.91-1.87, 1.87-1.83, 1.83-1.80, 1.80-1.77)*	50-1.98 (2.01-1.98)*	50-2.22 (2.26-2.22)*
R_{sym} or R_{merge}	7.5 (16.5, 18.3, 18.5, 18.8)	5.9 (22.2, 28.6, 30.4, 30.8, 32.7)	13.5 (70.9)	5.6 (16.4)
I/sI	19.8 (5.9, 5.4, 4.9, 4.5)	15.0 (3.5, 2.7, 2.4, 2.2, 2.0)	13.4 (2.8)	31.1 (10.6)
Completeness (%)	82.6 (54.8, 45.2, 34.0, 23.0)	74.1 (62.5, 49.8, 35.7, 20.9, 3.7)	100 (100)	99.6 (92.3)
Redundancy	5.6 (2.6, 2.4, 2.2, 2.0)	3.8 (2.1, 1.9, 1.7, 1.6, 1.4)	6.9 (6.7)	6.6 (4.4)
Refinement				
Resolution (Å)	30.21-2.30 (2.42-2.30)	26.78-1.77 (1.84-1.77)	43.42-1.98 (2.05-1.98)	35.84-2.22 (2.30-2.22)
No. reflections	18859	35657	34887	24496
R_{work}/R_{free}	23.67/26.82 (33.20/36.54)	19.06/23.71 (31.94/33.99)	16.75/20.39 (21.58/25.62)	18.32/20.91 (21.04/25.21)
No. atoms	3340	3690	3659	3526
Protein	3244	3282	3285	3258
Water	96	408	299	267
Ligand			75	1
B-factors (Å^2)	44.49	36.46	37.64	33.80
Protein	44.76	36.14	37.17	33.52
Water	35.28	39.04	40.48	37.26
Ligand			47.13	18.59
R.m.s deviations				
Bond lengths (Å)	0.003	0.006	0.005	0.005
Bond angles (°)	0.64	0.78	0.77	0.80
Ramachadran Favored %	96.0	97.0	97.0	96.5
Ramachadran Outliers %	0.0	0.0	0.0	0.00
MolProbity all-atoms clashscore	2.0	0.93	1.81	2.96
PDB ID	6B5P	6B5R	6B5S	6B5T

* Statistics for the highest-resolution shell are shown in parentheses. Fab, antigen-binding fragment.

e. Detailed interactions of peptide 25 with CIS43 antigen binding fragment heavy chain.

Peptide 25	HSDC	ASA	BSA
A:ASN 1		204.34	0.00
A:VAL 2		140.85	0.00
A:ASP 3	HS	85.41	25.29 |||
A:PRO 4		103.23	0.00
A:ASN 5		117.88	47.97 |||||
A:ALA 6		86.60	24.02 |||
A:ASN 7	H	69.29	41.73 ||||||
A:PRO 8		108.99	68.01 ||||||
A:ASN 9	H	136.99	126.00 |||||||||
A:VAL 10		107.06	40.74 ||||
A:ASP 11	H	188.81	44.16 |||

CIS43 Heavy	HSDC	ASA	BSA
H:TYR 32		73.01	4.87 |
H:ALA 33	H	31.39	28.22 |||||||||
H:HIS 35		30.84	22.87 |||||||
H:TRP 47		86.62	5.61 |
H:TRP 50		53.75	43.06 ||||||||
H:LYS 52		91.06	32.75 ||||
H:ARG 58	HS	159.04	55.37 ||||
H:LEU 95	H	45.54	10.84 |||
H:THR 96		83.39	27.92 ||||
H:VAL 97		25.86	18.59 |||||||
H:LEU 98	H	130.67	53.27 |||||
H:THR 99		73.05	6.36 |
H:PRO 100		138.92	16.24 |

Hydrogen Bonds

Peptide 25	Dist. [Å]	CIS43 Heavy chain
A:ASN 7[HD21]	2.12	H:LEU 95[O]
A:ASN 9[HD21]	2.01	H:ALA 33[O]
A:ASN 9[HD22]	2.40	H:LEU 95[O]
A:ASP 11[H]	2.33	H:LEU 98[O]
A:ASP 3[OD2]	2.43	H:ARG 58[HH12]
A:ASN 9[O]	2.25	H:LEU 98[H]
A:ASN 9[OD1]	2.04	H:ALA 33[H]

Salt Bridges

Peptide 25	Dist. [Å]	CIS43 Heavy chain
A:ASP 3[OD1]	3.81	H:ARG 58[NH1]
A:ASP 3[OD2]	3.07	H:ARG 58[NH1]
A:ASP 3[OD2]	3.22	H:ARG 58[NH2]

f. Detailed interactions of peptide 25 with Fab CIS43 Light chain.

Peptide 25	HSDC	ASA	BSA
A:ASN 1		204.34	49.19 |||
A:VAL 2		140.85	111.89 ||||||||
A:ASP 3	H	85.41	32.89 ||||
A:PRO 4		103.23	0.00
A:ASN 5		117.88	1.54 |
A:ALA 6		86.60	63.77 |||||||
A:ASN 7		69.29	27.11 ||||
A:PRO 8		108.99	0.00
A:ASN 9		136.99	0.00
A:VAL 10		107.06	64.61 ||||||
A:ASP 11		188.81	5.57 |

CIS43 Kappa	HSDC	ASA	BSA
L:TYR 27D		101.73	36.39 ||||
L:TYR 32		41.78	25.64 ||||||
L:TRP 50		72.61	19.70 |||
L:HIS 89		14.47	3.03 |||
L:TYR 91		60.81	37.89 ||||||
L:TYR 92	H	90.54	67.82 |||||||
L:SER 93		43.52	17.68 ||||
L:SER 94		103.17	40.15 ||||
L:LEU 96		104.68	35.83 ||||

Hydrogen Bonds

Peptide 25	Dist. [Å]	CIS43 Kappa
A:ASP 3[H]	2.15	L:TYR 92[O]

g. Detailed interactions of peptide 29 with Fab CIS43 Heavy chain.

Peptide 29	HSDC	ASA	BSA
A:ASN 3		152.02	0.00
A:PRO 4		112.17	0.00
A:ASN 5		157.68	1.97 |
A:ALA 6		77.61	11.11 ||
A:ASN 7	H	80.26	48.53 |||||||
A:PRO 8		129.13	78.52 |||||||
A:ASN 9	H	136.85	127.93 |||||||||
A:ALA 10		69.81	29.58 |||||
A:ASN 11		190.99	40.11 |||

CIS43 heavy chain	HSDC	ASA	BSA
H:TYR 32		70.79	8.03 ||
H:ALA 33	H	28.80	27.39 ||||||||
H:HIS 35		32.94	23.54 |||||||
H:TRP 50		53.65	33.85 |||||||
H:LYS 52		93.44	18.67 ||
H:LEU 94		0.45	0.45 |||||||||
H:LEU 95	H	42.46	10.80 |||
H:THR 96		89.48	29.30 ||||
H:VAL 97		18.02	15.73 |||||||
H:LEU 98	H	125.94	49.24 ||||
H:THR 99		67.65	4.33 |
H:PRO 100		142.86	11.88 |

Hydrogen Bonds

Peptide 29	Dist. [Å]	CIS43 heavy chain
A:ASN 7[HD21]	1.87	H:LEU 95[O]
A:ASN 9[HD21]	1.98	H:ALA 33[O]
A:ASN 9[O]	2.22	H:LEU 98[H]
A:ASN 9[OD1]	2.10	H:ALA 33[H]

h. Detailed interactions of peptide 29 with Fab CIS43 Light chain.

Peptide 29	HSDC	ASA	BSA
A:ASN 3		152.02	50.02 ||||
A:PRO 4		112.17	74.83 ||||||
A:ASN 5		157.68	49.31 ||||
A:ALA 6	H	77.61	62.66 ||||||||
A:ASN 7		80.26	31.73 ||||
A:PRO 8		129.13	0.00
A:ASN 9		136.85	0.00
A:ALA 10		69.81	40.23 |||||
A:ASN 11		190.99	44.54 |||

CIS43 Kappa	HSDC	ASA	BSA
L:TYR 27D		91.00	44.32 |||||
L:ASN 28		59.18	5.25 |
L:LYS 30		78.39	10.07 ||
L:TYR 32		42.26	33.09 |||||||
L:TRP 50		75.38	29.47 ||||
L:HIS 89		11.69	2.17 ||
L:TYR 91		57.24	33.66 |||||
L:TYR 92		87.31	59.89 ||||||
L:SER 93		43.13	15.12 ||||
L:SER 94	H	98.77	39.18 ||||
L:LEU 96		105.03	30.85 |||

Hydrogen Bonds

Peptide 29	Dist. [Å]	CIS43 light chain
A:ALA 6[O]	3.83	L:SER 94[OG]

ASA Accessible Surface Area, Å² **BSA** Buried Surface Area, Å² **HSDC** Hydrogen bond/Salt bridge/Disulphide bond/Covalent link

|||| Buried area percentage, one bar per 10% **Fab**, antigen-binding fragment.

Nature Medicine: doi:10.1038/nm.4512

Supplementary Table 4 Details of the interactions of CIS43 antigen-binding fragment with peptides 20, 21, 25, and 29 (from Pisa web server).

a. Detailed interactions of peptide 20 with Fab CIS43 Heavy chain.

Peptide 20	HSDC	ASA	BSA
-			
A:ASN 1		199.53	0.00
A:PRO 2		118.85	0.00
A:ASP 3	S	90.55	13.65 ||
A:PRO 4		110.37	0.00
A:ASN 5		121.53	52.07 |||||
A:ALA 6		89.92	24.79 |||
A:ASN 7	H	71.07	41.08 |||||
A:PRO 8		111.17	69.87 |||||||
A:ASN 9	H	137.53	131.64 |||||||||
A:VAL 10		162.15	52.29 ||||

CIS43 Heavy	HSDC	ASA	BSA
H:TYR 32		49.03	7.29 ||
H:ALA 33	H	27.96	26.05 |||||||||
H:HIS 35		32.22	23.42 |||||||
H:TRP 47		83.63	5.61 |
H:TRP 50		49.50	40.34 ||||||||
H:LYS 52		88.27	22.27 |||
H:ARG 58	S	155.23	70.57 |||||
H:LEU 95	H	47.07	11.42 |||
H:THR 96		86.35	25.23 ||||
H:VAL 97		13.22	13.22 |||||||||
H:LEU 98	H	134.90	45.59 ||||
H:THR 99		56.24	7.36 ||

Hydrogen Bonds

Peptide 20	Dist. [Å]	CIS43 Heavy
A:ASN 7[HD21]	1.92	H:LEU 95[O]
A:ASN 9[HD21]	2.16	H:ALA 33[O]
A:ASN 9[HD22]	2.38	H:LEU 95[O]
A:ASN 9[O]	2.06	H:LEU 98[H]
A:ASN 9[OD1]	1.89	H:ALA 33[H]

Salt Briges

Peptide 20	Dist. [Å]	CIS43 Heavy
A:ASP 3[OD1]	3.97	H:ARG 58[NH1]
A:ASP 3[OD2]	3.80	H:ARG 58[NH1]
A:ASP 3[OD2]	3.90	H:ARG 58[NH2]

b. Detailed interactions of peptide 20 with Fab CIS43 Light chain.

Peptide 20	HSDC	ASA	BSA
A:ASN 1		199.53	57.13 |||
A:PRO 2		118.85	97.83 ||||||||
A:ASP 3	H	90.55	28.99 ||||
A:PRO 4		110.37	0.00
A:ASN 5		121.53	1.68 |
A:ALA 6		89.92	65.12 |||||||
A:ASN 7		71.07	29.99 |||||
A:PRO 8		111.17	0.00
A:ASN 9		137.53	0.00
A:VAL 10		162.15	65.76 |||||

CIS43 Kappa	HSDC	ASA	BSA
L:TYR 27D		109.98	47.82 ||||
L:TYR 32		44.44	22.80 |||||
L:TRP 50		83.84	15.63 ||
L:TYR 91		63.53	38.40 ||||||
L:TYR 92	H	82.09	69.83 ||||||||
L:SER 93		39.00	10.15 |||
L:SER 94		101.58	34.26 ||||
L:LEU 96		109.67	39.66 ||||

Hydrogen Bonds

Peptide 20	Dist. [Å]	CIS43 Kappa
A:ASP 3[H]	2.09	L:TYR 92[O]

c. Detailed interactions of peptide 21 with Fab CIS43 Heavy chain.

Peptide 21	HSDC	ASA	BSA
A:ASN 1		194.02	0.00
A:PRO 2		120.14	0.00
A:ASP 3	HS	93.11	17.94 ||
A:PRO 4		87.09	0.00
A:ASN 5		123.25	45.86 ||||
A:ALA 6		88.01	25.03 |||
A:ASN 7	H	69.29	40.59 ||||||
A:PRO 8		114.61	73.02 |||||||
A:ASN 9	H	135.47	127.77 |||||||||
A:VAL 10		92.43	37.13 ||||
A:ASP 11	H	96.40	49.84 |||||
A:PRO 12		102.27	0.00
A:ASN 13		166.91	19.49 ||

CIS43 Heavy	HSDC	ASA	BSA
H:TYR 32		56.26	8.63 ||
H:ALA 33	H	26.67	25.54 |||||||||
H:HIS 35		29.20	21.26 |||||||
H:TRP 47		88.95	5.74 |
H:TRP 50		51.96	40.63 ||||||||
H:LYS 52		88.24	26.49 || ||
H:ARG 58	HS	155.20	63.65 |||||
H:LEU 95	H	44.74	11.66 |||
H:THR 96		89.74	27.30 ||||
H:VAL 97		13.56	113.56 |||||||||
H:LEU 98	H	135.94	55.85 ||||
H:THR 99		47.76	10.46 |||
H:PRO 100		141.94	33.54 |||

Hydrogen Bonds

Peptide 21	Dist. [Å]	CIS43 Heavy chain
A:ASN 7[HD21]	2.16	H:LEU 95[O]
A:ASN 9[HD21]	1.94	H:ALA 33[O]
A:ASN 9[HD22]	2.47	H:LEU 95[O]
A:ASP 11[H]	1.95	H:LEU 98[O]
A:ASP 3[OD2]	2.46	H:ARG 58[HH12]
A:ASN 9[O]	2.30	H:LEU 98[H]
A:ASN 9[OD1]	1.87	H:ALA 33[H]

Salt Bridges

Peptide 21	Dist. [Å]	CIS43 Heavy chain
A:ASP 3[OD2]	3.27	H:ARG 58[NH1]
A:ASP 3[OD2]	3.73	H:ARG 58[NH2]

d. Detailed interactions of peptide 21 with Fab CIS43 Light chain.

Peptide 21	HSDC	ASA	BSA
A:ASN 1	H	194.02	54.57 |||
A:PRO 2		120.14	100.05 ||||||||
A:ASP 3	H	93.11	34.37 ||||
A:PRO 4		87.09	0.00
A:ASN 5		123.25	1.12 |
A:ALA 6		88.01	62.98 |||||||
A:ASN 7		69.29	28.70 |||||
A:PRO 8		114.61	0.00
A:ASN 9		135.47	0.00
A:VAL 10		92.43	50.05 ||||||
A:ASP 11		96.40	4.54 |
A:PRO 12		102.27	55.27 ||||||
A:ASN 13		166.91	21.93 ||

CIS43 Kappa	HSDC	ASA	BSA
L:TYR 27D		109.91	48.68 |||||
L:ASN 28		58.73	17.46 ||||
L:LYS 30		78.55	23.86 |||
L:TYR 32		42.77	37.02 ||||||||
L:TRP 50		82.72	35.24 ||||
L:HIS 89		12.98	2.14 ||
L:TYR 91		63.55	40.01 ||||||
L:TYR 92	H	88.13	69.67 ||||||||
L:SER 93		42.00	14.88 |||
L:SER 94		105.57	35.12 |||||
L:LEU 96		106.03	37.79 ||||

Hydrogen Bonds

Peptide 21	Dist. [Å]	CIS43 Kappa
A:ASN 1[H2]	2.42	L:TYR 92[OH
A:ASP 3[H]	1.90	L:TYR 92[O]

ASA Accessible Surface Area, Å² **BSA** Buried Surface Area, Å² **HSDC** Hydrogen bond/Salt bridge/Disulphide bond/Covalent link

|||| Buried area percentage, one bar per 10% **Fab**, antigen-binding fragment.

Nature Medicine: doi:10.1038/nm.4512

Supplementary Table 3 Data collection and refinement statistics for CIS43 antigen-binding fragment.

	CIS43 Fab with peptide 20	CIS43 Fab with peptide 21	CIS43 Fab with peptide 25	CIS43 Fab with peptide 29
Data collection				
Space group	C2	C2	C2	C2
Cell dimensions				
a, *b*, *c* (Å)	93.94, 61.67, 75.37	93.48, 61.86, 75.06	93.07, 60.42, 83.31	93.24, 60.41, 84.84
α, β, γ (°)	90.00, 106.04, 90.00	90.00, 105.51, 90.00	90.00, 102.83, 90.00	90.00, 107.02, 90.00
Resolution (Å)	50-2.40 (2.44-2.40)*	50-1.79 (1.82-1.79)*	50-1.98 (2.01-1.98)*	50-2.18 (2.22-2.18)*
R_{sym} or R_{merge}	15.4 (31.3)	10.3 (33.8)	8.8 (55.2)	14.7 (56.1)
I/s*I*	6.1 (2.4)	9.6 (2.4)	13.9 (2.2)	13.5 (1.5)
Completeness (%)	93.3 (75.1)	94.7 (97.9)	99.6 (92.7)	98.7 (85.4)
Redundancy	2.9 (2.2)	3.2 (2.7)	3.7 (3.3)	6.2 (3.7)
Refinement				
Resolution (Å)	45.14-2.40 (2.48-2.40)	39.00-1.79 (1.83-1.79)	40.61-1.98 (2.05-1.98)	46.09-2.19 (2.27-2.19)
No. reflections	15362	37098	31443	22789
R_{work}/R_{free}	19.85/23.78 (25.79/30.24)	20.67/23.47 (27.90/31.20)	17.45/20.94 (23.15-28.10)	19.29/24.01 (28.64/34.48)
No. atoms	3473	3778	3673	3546
Protein	3408	3433	3459	3422
Water	65	321	214	124
Ligand		24		
B-factors (Å^2)	50.0	41.1	43.8	52.5
Protein	50.1	40.5	43.9	52.7
Water	40.8	42.5	41.0	47.35
Ligand		101.3		
R.m.s deviations				
Bond lengths (Å)	0.006	0.003	0.005	0.002
Bond angles (°)	0.82	0.72	0.77	0.61
Ramachadran Favored %	97.5	98.0	98.0	95.3
Ramachadran Outliers %	0.0	0.0	0.0	0.0
MolProbity all-atoms clashscore	1.78	6.17	3.22	1.33
PDB ID	6B5L	6B5M	6B5N	6B5O

* Statistics for the highest-resolution shell are shown in parentheses. Fab, antigen-binding fragment.

Supplementary Table 2 Biolayer interferometry kinetics of PfCSP antibodies binding to rPfCSP, Peptide 21, or Peptide 29.

a **PfCSP** (sensor)

Antibody	K_D (M)	K_D Error	k_{on} (1/Ms)	k_{on} Error	k_{dis} (1/s)	k_{dis} Error
2A10	1.50E-10	1.47E-11	1.11E+05	2.48E+03	1.66E-05	1.59E-06
CIS06	n/a	n/a	n/a	n/a	n/a	n/a
CIS23	1.55E-09	7.19E-11	1.91E+05	8.60E+03	2.96E-04	3.08E-06
CIS34	1.50E-09	7.74E-11	1.55E+05	7.32E+03	2.33E-04	4.78E-06
CIS42	6.72E-10	1.92E-11	1.53E+05	3.15E+03	1.03E-04	2.04E-06
CIS43	9.12E-10	8.24E-11	1.47E+05	1.24E+04	1.34E-04	4.22E-06

b **Peptide 21** (sensor)

Antibody	K_D (M)	K_D Error	k_{on} (1/Ms)	k_{on} Error	k_{dis} (1/s)	k_{dis} Error
2A10	5.79E-11	7.26E-12	2.69E+05	3.22E+03	1.56E-05	1.94E-06
CIS06	n/a	n/a	n/a	n/a	n/a	n/a
CIS23	6.06E-09	9.48E-10	6.21E+06	9.25E+05	3.76E-02	1.80E-03
CIS34	9.26E-11	1.80E-11	5.72E+05	1.80E+04	5.30E-05	1.02E-05
CIS42	1.69E-09	9.39E-11	4.20E+05	2.28E+04	7.09E-04	8.47E-06
CIS43	<1.0E-12	1.14E-11	2.45E+05	4.61E+03	<1.0E-07	n.d.

c **Peptide 29** (sensor)

Antibody	K_D (M)	K_D Error	k_{on} (1/Ms)	k_{on} Error	k_{dis} (1/s)	k_{dis} Error
2A10	1.77E-09	7.12E-11	6.66E+05	2.61E+04	1.18E-03	1.03E-05
CIS06	n/a	n/a	n/a	n/a	n/a	n/a
CIS23	2.18E-09	1.16E-10	6.91E+05	3.60E+04	1.50E-03	1.54E-05
CIS34	1.03E-09	4.76E-11	5.86E+05	2.56E+04	6.05E-04	9.19E-06
CIS42	2.21E-09	2.80E-10	3.36E+06	4.09E+05	7.43E-03	2.69E-04
CIS43	4.66E-09	3.88E-10	1.39E+06	1.13E+05	6.46E-03	9.94E-05

Errors are from model fitting.
K_D, affinity constant. K_D indicates the ratio of the association rate constant (k_{on}) to the dissociation rate constant (k_{dis}).

Supplementary Table 1 PfCSP Immunoglobulin V-gene family usage.

Antibody	V_H	V_H maturation (nt, %)	D	J_H	CDRH3 length (aa)	V_L	V_L maturation (%)	J_L
CIS06	VH1-58*01	4.2	DH1-1*01	JH5*02	14	Vκ1-39*01	11.1	Jκ2*01
CIS23	VH3-30*03	2.1	DH6-13*01	JH4*02	15	Vκ3-11*01	1.9	Jκ2*01
CIS34	VH3-33*01	2.8	DH6-13*13	JH5*02	17	Vκ1-39*01	3.7	Jκ3*01
CIS42	VH7-4-1*02	3.1	DH5-18*01	JH4*02	12	Vλ2-23*02	3.5	Jλ3*02
CIS43	VH1-3*01	3.8	DH4-23*01	JH3*02	14	Vκ4-1*01	2.9	Jκ4*01
mAb04	VH3~33*01	2.0	DH3~22*01	JH4*02	16	Vκ2D~29*01	0.0	Jκ2*01
mAb09	VH3~33*01	3.1	DH3~22*01	JH3*02	15	Vκ3~11*01	1.4	Jκ3*01
mAb10	VH3~33*01,04	3.3	DH4~23*01	JH4*02	16	Vκ1~5*01	1.7	Jκ1*01
mAb15	VH3~33*01	0.2	DH3~22*01	JH6*02	22	Vκ3~20*01	0.3	Jκ1*01
mAb19	VH6~1*01	1.1	DH2~2*01	JH1*01	13	Vκ4~1*01	1.1	Jκ4*01
mAb21	VH3~30*04	2.9	DH2~IR2*01	JH3*02	10	Vλ2~8*01	0.6	Jλ1*01
mAb22	VH3~33*01	0.5	DH2~21*02	JH4*02	19	Vκ3~20*01	0.0	Jκ3*01
mAb25	VH3~33*01	1.7	DH6~13*01	JH3*02	19	Vκ1~5*03	1.2	Jκ1*01
mAb26	VH3~48*03	0.7	DH2~2*01	JH4*02	18	Vκ1~5*03	0.3	Jκ1*01
mAb27	VH3~49*03	0.8	DH6~13*01	JH4*02	12	Vκ3~15*01	0.3	Jκ1*01
mAb28	VH4~34*12	3.7	DH4~17*01	JH4*02	13	Vκ1D~17*01	2.0	Jκ4*01
mAb30	VH3~33*01	1.5	DH4~17*01	JH4*02	16	Vκ1~5*03	0.0	Jκ1*01

V, variable region; H, heavy chain; L, light chain; κ, Kappa; λ,Lambda; nt, nucleotides; aa, amino acid. Yellow-highlighted, antibodies isolated from PfCSP-specific memory B cells. Non-highlighted, antibodies isolated from plasmablasts.

a

Plasmodium falciparum NF54 strain | PfCSP sequence

MMRKLAILSVSSFLFVEALFQEYQCYGSSSNTRVLNELNYDNAGTNLYNELEMNYYGKQENWYSLKKNSRSLGENDDGNNEDNEKL
RKPKHKKLKQPADGNPDPNANPNVDPNANPNVDPNANPNVDPNANPNANPNANPNANPNANPNANPNANPNANPNANPNANPNA
NPNANPNANPNANPNANPNANPNANPNVDPNANPNANPNANPNANPNANPNANPNANPNANPNANPNANPNANPNANPNANPNA
NPNANPNANPNANPNANPNKNNQGNGQGHNMPNDPNRNVDENANANSAVKNNNNEEPSDKHIKEYLNKIQNSLSTEWSPCSVTC
GNGIQVRIKPGSANKPKDELDYANDIEKKICKMEKCSSVFNVVNSSIGLIMVLSFLFLN

Signal sequence-N-terminus-Repeat-C-terminus-GPI anchor

RI Peptide 21

NF54: 90-KHKKLKQPADGNPDPNANPNVDPNAN-115

b

Position	101	102	103	104	105	106	107	108	109	110	111	112	113	114	115
NF54 Sequence	N	P	D	P	N	A	N	P	N	V	D	P	N	A	N

Database/Study [ref]	Isolates Studied	Polymorphism	Allele Frequency	Location
Lab/Vaccine Strains [29, 47]	NF54/3D7/NF7/GB4/RO33/WC			Africa
	7G8/HB3			S. America
	K1/Dd2/MAD20/FCC-1/HN/837			Asia
Pf3K Database [30]		V110A®	1/5258	Ghana
		D111N®	1/5260	Ghana
		P102V✓	1/5264	Thailand
	All others		5263/5266	*Multiple Africa/Asia
India Study [48]	-	D111V	1/161	India
	-	103DP104 > 103VL104	1/161	India
	-	P102A	1/161	India
	-	N105P	1/161	India
	-	N105H	1/161	India
	All others		156/161	India
Iran Study [49]	All isolates		21/21	Iran
Genetic Diversity Study [50]	All isolates		472/472	#Multiple Africa/Asia

*Countries included in Pf3k Database: The Gambia, Guinea, Ghana, Mali, Malawi, DR Congo, Nigeria, Senegal, Thailand, Cambodia, Bangledesh, Vietnam, Myanmar, Laos

#Countries in Genetic Diversity Study: Tanzania, Ghana, Thailand, Philippines, Papua New Guinea, Solomon Islands, Vanuatu

®unclear if on same allele or not
✓not enough reads to be confident of SNP

c

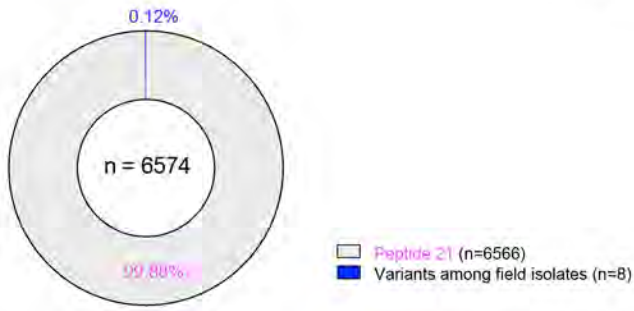

Supplementary Figure 11 Peptide 21 sequence conservation.

a, Complete PfCSP sequence of NF54 strain (clone 3D7). Central repeat region (in black) is flanked by the N- (blue) and C- (green) terminal regions, the leader (grey) and GPI anchor (orange) sequences. Boxed in magenta is peptide 21 sequence which occurs at the junction of the N- and Repeat regions. RI sequence is in brown letters. **b,** Peptide 21 sequence variation among laboratory and field isolates. Each residue within NF54 peptide 21 sequence is depicted with its position on top. Non-synonymous single nucleotide polymorphisms (SNPs) or indels leading to amino acid coding changes are shown with their respective frequencies, and geographic locations. **c,** Pie chart representing frequencies of peptide 21 amino acid conservation shown in **b** (see URLs)[38-42].

Nature Medicine: doi:10.1038/nm.4512

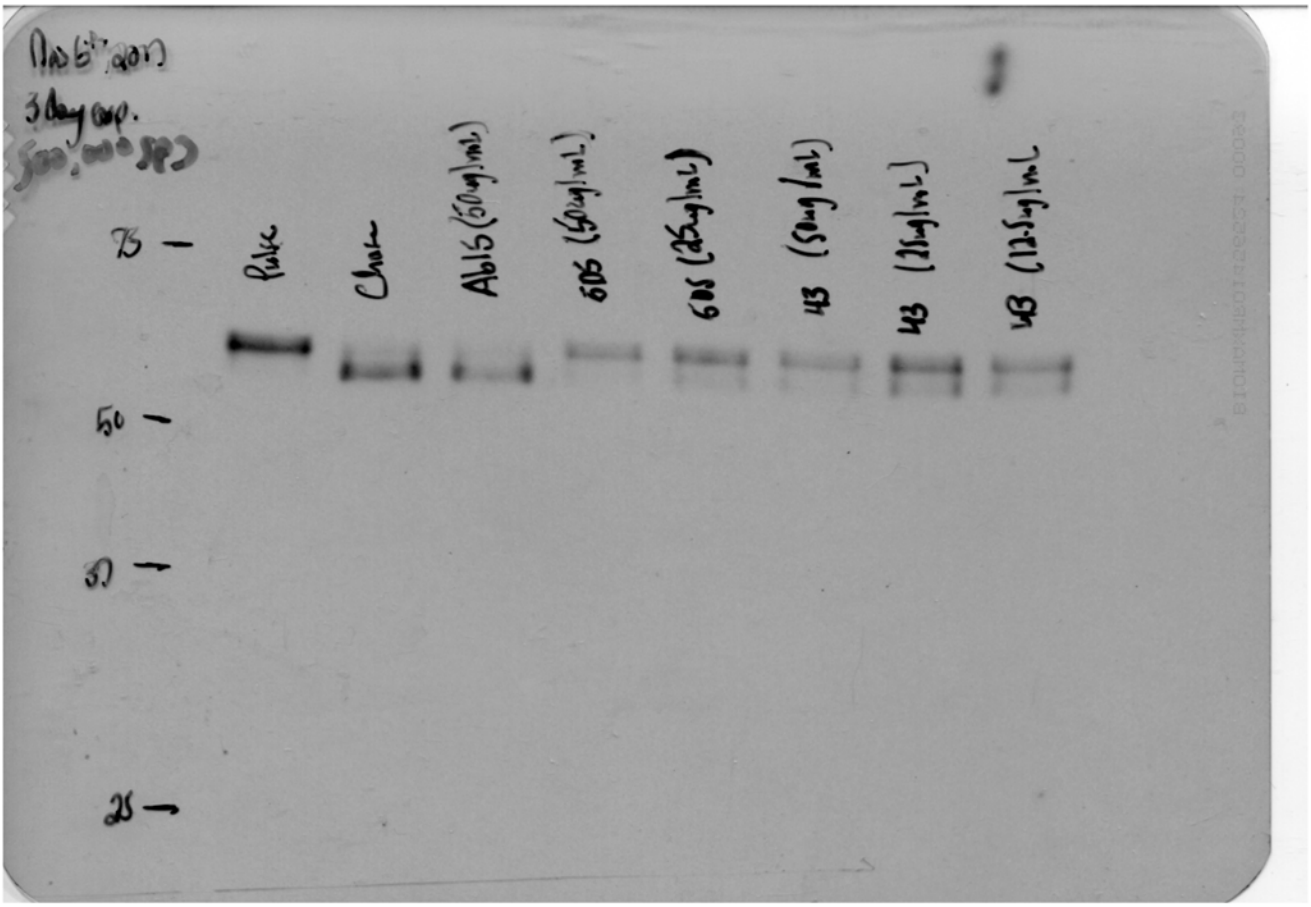

Supplementary Figure 10 Western blot used in Figure 5.
Concentrations (μg/ml) of monoclonal antibodies are indicated on top of the autoradiograph. Pulse, Chase, mAb15 (human anti-C terminus PfCSP antibody used as negative control); 5D5 (mouse anti-N terminus PfCSP antibody used as positive control for cleavage of PfCSP on PfSPZ); 43 (CIS43). Molecular mass is indicated in kilodaltons on the left side of the autoradiograph.

a

```
Peptide 20   NPDPNANPN
Peptide 21   NPDPNANPNVDPN
Peptide 25   NVDPNANPNVD
Peptide 29     NPNANPNAN
               1st  2nd  3rd
```

CIS43 Fab

Peptide 20

Phi, Psi (°)	1st	2nd	3rd
N1/D	-92, 115	-135, 111	NA
P	-63, -18	-66, -10	NA
N2	-92, -4	-85, 0	NA
A/V	-58, -51	NA	NA

Peptide 21

1st	2nd	3rd
-96, 105	-138, 100	-91, 106
-63, -14	-53, -25	-66, -15
-92, -1	-69, -14	NA
-60, -43	-92, 119	NA

Peptide 25

1st	2nd	3rd
-100, 111	-144, 108	NA
-69, -14	-68, -12	NA
-100, 6	-74, -12	NA
-57, -43	-94, 118	NA

Peptide 29

1st	2nd	3rd
NA	-141, 107	NA
-100, 121	-44, -25	NA
-60, -63	-75, -26	NA
-70, -141	-82, 103	NA

b

```
Peptide 20     NPDPNANPNVD
Peptide 21     NPDPNANPNVDPN
Peptide 25     NVDPNANPNVDPN
Peptide 29   ANPNANPNANPNA
               1st  2nd  3rd  4th
```

CIS42 Fab

Peptide 20

Phi, Psi (°)	1st	2nd	3rd
N1/D	NA	-79, 132	-93, 123
P	NA	-68, -24	-71, -12
N2	NA	-82, -15	-84, 60
A/V	NA	-64, 140	-77, 158

Peptide 21

2nd	3rd	4th
-61, 125	-111, 121	-73, 123
-61, -25	-67, -18	-79, -3
-83, -9	-87, 67	
-75, 162	-134, 159	

Peptide 25

2nd	3rd	4th
-86, 117	-100, 118	-65, 120
-64, -24	-65, -19	-89, 26
-85, -8	-80, 0	
-73, 151	-65, 145	

Peptide 29

1st	2nd	3rd
51, 60	-69, 122	-101, 117
-71, -24	-61, -27	-65, -20
-91, -66	-80, -15	-78, 61
-68, 153	-70, 149	

c

	Phi, Psi (°)
N	-99 ± 26, 113 ± 15
P	-68 ± 12, -16 ± 12
N	-82 ± 10, -12 ± 17
A	-76 ± 20, 142 ± 20

d

	Phi, Psi (°)
N	-69, 118
P	-71, -6
N	-110, -16
A	-80, 165

Supplementary Figure 9 Structural repeat motif analysis.
Phi and Psi angles (°) for residues N/D, P, N and A/V of the repeat motif for **a,** PfCSP peptides bound to CIS43 antigen-binding fragment; **b,** PfCSP peptides bound to CIS42 antigen-binding fragment; **c,** Average plus/minus one standard deviation for **a** and **b**; and **d,** Crystal structure of NPNA determined by Ghasparian et al.[33]. The alignment of the repeat motif peptide, based on the crystal structures as described in Fig. 4 and Supplementary Fig. 6, are shown as indicated. The NPN repeat motif occurrences are underlined under the sequences. Highlighted in red are the notable outliers for which Phi and/ or Psi is 60° different compared to others in the same row. For peptides bound to CIS43 antigen-binding fragment, this difference is in the first A/V, leading to a repeating structure of NPNA-NPNA; for peptides bound to CIS42 antigen-binding fragment, this difference is with N2 (the Asn following the Pro), leading to a repeating structure of ANPN-ANPN. We note that the Phi, Psi angles for the 1st occurrence of the NPN repeat in peptide 29 bound to CIS43 differs from the rest as shown in Fig. 4.

Nature Medicine: doi:10.1038/nm.4512

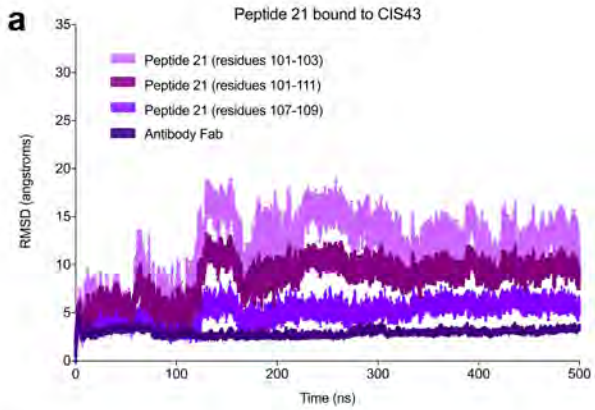

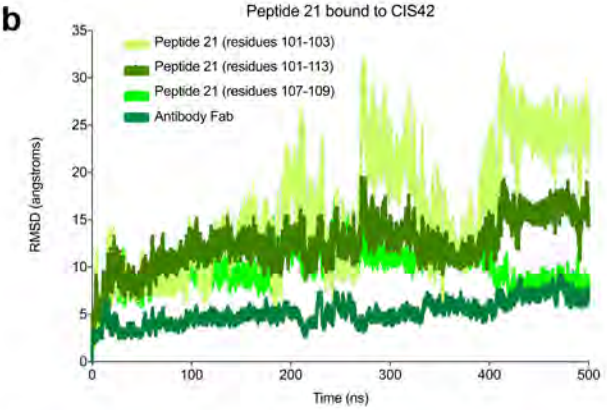

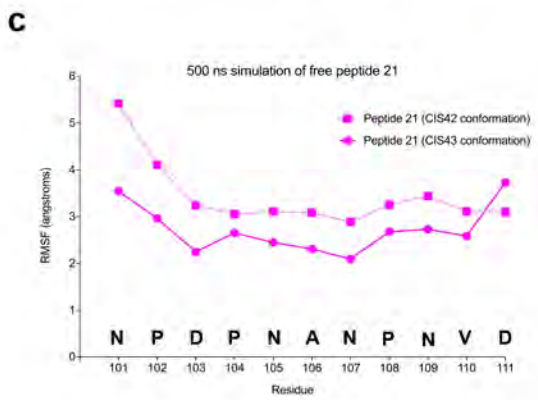

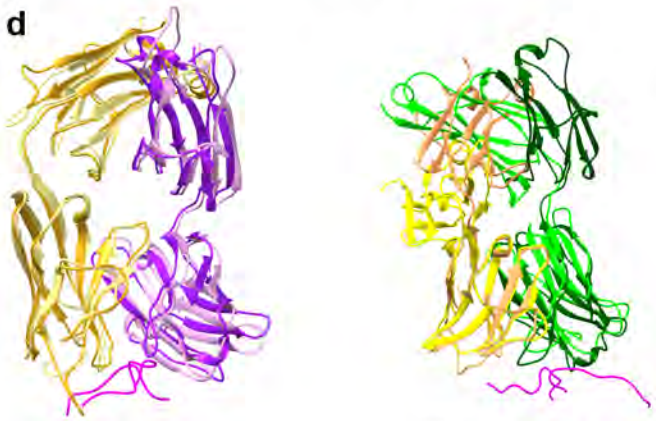

CIS43 bound to peptide 21
(crystal vs 500 ns)
2.96 Å RMSD

CIS42 bound to peptide 21
(crystal vs 500 ns)
7.48 Å RMSD

e

Time (ns)	CIS43 Fab	CIS42 Fab
	Number of hydrogen bonds	
Crystal	8	5
50	5 (3)	4 (1)
250	12 (2)	2 (0)
500	9 (1)	2 (0)

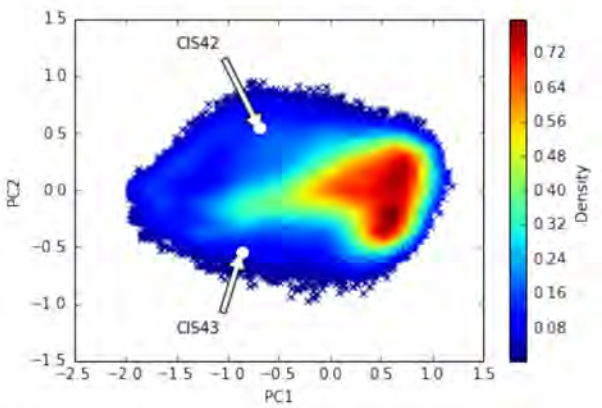

PC1	46.47
PC2	12.82
PC3	8.39
PC4	5.67
PC5	3.88
PC6	3.34
PC7	3.04
PC8	2.18
PC9	1.80
PC10	1.54

Supplementary Figure 8 Molecular Dynamics (MD) Simulations.
a, RMSD for CIS43 antigen-binding fragment bound to peptide 21over 500 nanoseconds (ns) of MD. CIS43 antigen-binding fragment heavy and light chain were used to align the trajectories. CIS43 antigen-binding fragment is depicted in indigo; full peptide 21 (residues 101-111) is depicted in plum; residues 107-109 in grape; and residues 101-103 in lavender. **b,** RMSD of CIS42 antigen-binding fragment bound to peptide 21 over 500 ns of MD, calculated the same as in a. CIS42 antigen-binding fragment is depicted in dark green; full peptide 21 (residues 101-113) is depicted in forest green; residues 107-109 in mint; and residues 101-103 in lime. **c,** RMSF of 500 ns of free peptide 21 beginning from its CIS43 antigen-binding fragment conformation (depicted in magenta circles and a solid line) and RMSF of free peptide 21 beginning from its CIS42 antigen-binding fragment conformation (depicted in magenta squares with a dotted line). **d,** CIS43 and CIS42 antigen-binding fragment crystal structures aligned to their 500 ns frames respectively. Color key for CIS43 antigen-binding fragment: crystal heavy chain shown in purple and crystal light chain shown in gold; 500 ns heavy chain shown in lavender and 500 ns light chain shown in khaki. Color key for CIS42 antigen-binding fragment: crystal heavy chain shown in dark green and crystal light chain shown in sandy brown; 500 ns heavy chain shown in bright green and 500 ns light chain shown in yellow. **e,** Hydrogen bonding analysis of peptide 21 in complex with CIS42 and CIS43 antigen-binding fragments over 500ns compared to the respective crystal structures. Hydrogen bonds were calculated between peptide residues and the antigen-binding fragment binding interface. Numbers in parentheses indicate bonds present in the crystal structure. **f,** Principal component analysis (PCA) of 500 ns of free peptide 21 colored by the number of times specific conformations occur. PC1 is plotted on the x-axis and PC2 is plotted on the y-axis. Crystal structures of peptide 21 in CIS42 and CIS43 antigen-binding fragment conformations are labeled with gray arrows. The top ten eigen values from the PCA analyses are listed in the table. n = 50,000.